Localized Breaking of Flux Surfaces and the Equilibrium β Limit in the W7AS Stellarator

A. Reiman, M.C. Zarnstorff, D. Monticello, J. Krommes
Princeton Plasma Physics Laboratory, Princeton, NJ 08543 USA
email address of main author*: reiman@pppl.gov*

A. Weller, J. Geiger, and the W7-AS Team
Max-Planck Institute for Plasma Physics, EURATOM Assoc., D-17491 Greifswald, Germany

Abstract. Calculations are presented for two W7AS shots which differ only in the magnitude of the current in the divertor control coil, but differ greatly in the experimentally attainable value of β ($\langle\beta\rangle \approx 2.7\%$ vs. $\langle\beta\rangle \approx 1.8\%$). Equilibrium calculations find that a region of chaotic magnetic field line trajectories fills approximately the outer 1/3 of the cross section in each of these configurations. The field lines in the stochastic region are calculated to behave as if the flux surfaces are broken only locally near the outer midplane and are preserved elsewhere. The calculated magnetic field line diffusion coefficients for the two shots, and the corresponding estimates of the contribution of field line stochasticity to thermal transport, are consistent with the observed differences in the attainable β, and also consistent with the differences in the reconstructed pressure profiles.

1. Introduction

It has been assumed since the early days of the fusion program that there is an equilibrium β limit in stellarators associated with breaking of the flux surfaces.[1] The intuition is that when the Shafranov shift becomes sufficiently large, the compression of the 3D flux surfaces on the outboard side of the plasma will break the flux surfaces. Only in recent years have stellarators achieved values of β sufficiently high to test this intuition, and to allow a systematic investigation of the equilibrium β limit. Both the W7AS and LHD stellarators exhibit degraded confinement at high values of β that does not appear to be caused by instabilities, [2,3] and the confinement degradation is correlated with a loss of flux surfaces in the outer region of the plasma calculated by the PIES and HINT three-dimensional equilibrium codes. This paper reports on the results of a more detailed comparison between W7AS experimental observations and PIES calculations for two shots.

A discovery that has emerged from the PIES calculations for W7AS is that the field lines in the stochastic region are calculated to behave as if the flux surfaces are broken only locally near the outer midplane and are preserved elsewhere. This differs from the picture conventionally assumed for regions of chaotic magnetic field lines, where the field lines are assumed to be everywhere diffusing radially. (See e.g. Ref. 5.) These PIES results are consistent with the intuition that the breaking of the flux surfaces is produced by the strong compression and distortion of the magnetic flux surfaces near the outer midplane caused by the Shafranov shift. Note that these surface remnants are quite different from cantori, which are special surface remnants with noble magnetic winding number that can restrict the diffusion of the magnetic field lines. Unlike cantori, the behavior we observe is exhibited by essentially all of the chaotic magnetic field line trajectories, and can therefore present a more formidable barrier to magnetic field line diffusion.

In both W7AS and LHD, the computationally predicted regions of stochastic field lines are observed to support substantial pressure gradients. We will see below that this is consistent with estimates of the contribution of the field line stochasticity to the radial transport. In analyzing the stochastic field line regions it is necessary to calculate the three-dimensional equilibrium solution, including the Pfirsch-Schlüter currents, in these regions. As we will

discuss below, this poses several subtleties, including the issue of how to calculate magnetic differential equations along chaotic field line trajectories. We will see below that the equations are mathematically equivalent to equations that arise in the resonance-broadening theory of plasma turbulence.

2. W7AS Divertor Control Coils and their Effect on β

W7AS has a set of divertor control coils which were designed to provide control over the resonant magnetic field near the plasma edge, for control of the edge islands in studies of island divertors. For the vacuum magnetic field corresponding to the shots we will study here, which has $\iota \approx$ ½ at the edge, the configuration is bounded by a well defined set of islands when the divertor control coil current $I_{cc} = 0$, and these edge islands can be suppressed by a divertor control coil current $I_{cc} = -0.7$ kA, so that the field then has nested flux surfaces out to the divertor plates. This suggested the use of the control coils in high β shots to provide a larger volume of nested flux surfaces, potentially allowing the machine to achieve higher values of β.

Figure 1 shows the maximum $\langle\beta\rangle$ achieved in four W7AS shots which differed only in the magnitude of the divertor control coil current. The highest $\langle\beta\rangle$ was achieved at a value of $I_{CC} / I_M \approx 0.15$, corresponding to $I_{CC} \approx -2.5$ kA, over three times the current that produces the largest flux surface volume at β = 0. To understand the finite β effects that determine the optimal value of I_{CC}, it is desirable to use a three-dimensional equilibrium code that can handle islands and stochastic regions. We have used the PIES code[4] for that purpose. In this paper we examine the results of PIES code calculations for the shots having $I_{CC} = 0$ and $I_{CC} \approx -2.5$ kA.

3. W7AS Modeling using Experimentally Determined Pressure and Current Profiles

Our modeling began with an optimized equilibrium reconstruction[2] based on the VMEC[6] three-dimensional equilibrium code, which assumes nested flux surfaces. Given specified coil currents, VMEC was used to calculate corresponding free-boundary equilibria for candidate pressure and current profiles, and a set of corresponding diagnostic data was calculated for comparison with the experimental data. The pressure and current profiles of the equilibria were adjusted to optimize the fit to the Thomson scattering data as well as to the data from the magnetic diagnostics. Our earlier modeling of the two shots examined in this paper assumed zero net current within each flux surface,[2] and optimized the fit to the Thomson data. To obtain an adequate fit also to the data from the magnetic diagnostics, it is necessary to allow a finite net current, and to adjust its profile accordingly.
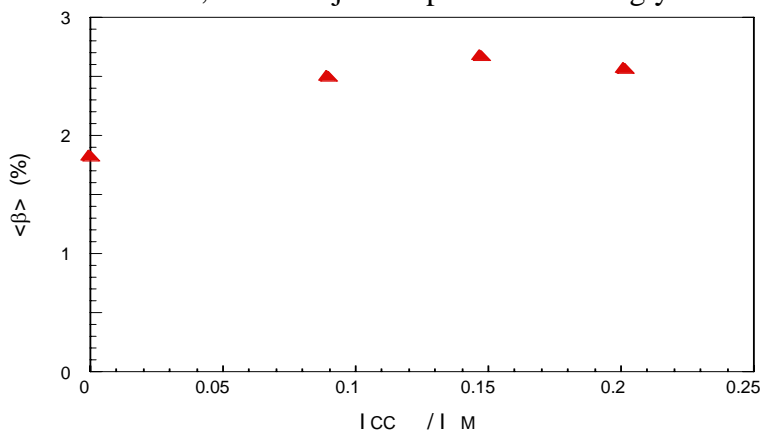

FIG. 1. Variation of achievable $\langle\beta\rangle$ versus the divertor control-coil current I_{CC} normalized by the modular coil current, for B=1.25 T, $P_{NB} = 2.8$ MW absorbed and $\iota_{vac} = 0.44$.

The VMEC equilibrium solution is used as the starting point for the calculation with the PIES code, which does not assume good flux surfaces. Having found the pressure and current profiles that provide an optimal fit to the experimental data, we keep these profiles fixed as the PIES code iterates, even when large stochastic regions appear at the plasma edge. In order to do that, we need to develop a corresponding equilibrium model for the stochastic regions.

4. Plasma Equilibrium in Regions of Chaotic Magnetic Field Line Trajectories

We assume that the magnetic field consists of two pieces, a piece with good flux surfaces, plus a relatively small resonant perturbation that produces chaotic field line trajectories and causes the magnetic field lines to slowly diffuse radially. The perturbation contributes to transport, and it can substantially affect the magnitude of the pressure gradient, but it is assumed to have only a small effect on the shape of the isobaric surfaces.

The MHD force balance equation, $\mathbf{j} \times \mathbf{B} = \nabla p$, implies that $\mathbf{B} \cdot \nabla p = 0$, which in turn implies that the pressure gradient must vanish in a stochastic region. We would like to allow finite pressure gradients in our stochastic regions, so we cannot satisfy the MHD equilibrium equations per se. However, consider a tensor pressure, $\boldsymbol{P} = p\boldsymbol{1} + \boldsymbol{\pi}$, with $|\nabla \cdot \boldsymbol{\pi}| << \nabla p$. Taking the dot product of $\mathbf{B}$ with the force balance equation we now get $\mathbf{B} \cdot \nabla p = -\mathbf{B} \cdot (\nabla \cdot \boldsymbol{\pi})$. If the field lines diffuse slowly in the radial direction, the pressure gradient along the field lines is small, and it can be balanced by a small tensor component of the pressure. (The same role could be played by a weak flow.) The solution of the equation along the field lines can be regarded as part of the transport problem, and we will see that it does not enter into the self-consistent solution for the magnetic field using the other components of the force balance equation.

Taking the cross product of $\mathbf{B}$ with the force balance equation we obtain an expression for $\mathbf{j}_\perp$, the component of the current density perpendicular to the magnetic field,

$$\mathbf{j}_\perp = \mathbf{B} \times \nabla p / B^2 + \mathbf{B} \times (\nabla \cdot \boldsymbol{\pi}) / B^2 \approx \mathbf{B} \times \nabla p / B^2, \qquad (1)$$

The component of $\mathbf{j}$ parallel to the magnetic field, $j_\parallel$, is determined from $\nabla \cdot \mathbf{j} = 0$, which gives the 1D equation along the field line ("magnetic differential equation")

$$\mathbf{B} \cdot \nabla (j_\parallel / B) = -\nabla \cdot \mathbf{j}_\perp. \qquad (2)$$

The equations are closed by Ampere's Law: $\nabla \times \mathbf{B} = \mathbf{j}$. Equations (1) and (2) specify $\mathbf{j}$ as a function of $\mathbf{B}$, $\mathbf{j} = \mathbf{j}(\mathbf{B})$. We have therefore recast the equilibrium equations in the form

$$\nabla \times \mathbf{B} = \mathbf{j}(\mathbf{B}). \qquad (3)$$

This is the form in which the equations are solved by the PIES code.

In practice, Eq. (1) gives an explicit expression for $\mathbf{j}_\perp$, and Eq. (3) can be solved by inverting a matrix which represents the curl operator. (We finite difference in the radial direction and use a Fourier representation in the θ and ϕ directions.) The magnetic differential equation, Eq. (2), presents subtle issues, particularly when the field line trajectories are chaotic. We first discuss the case with good flux surfaces, and then turn to the difficulties posed by chaotic field line trajectories.

On a good flux surface, Eq. (2) can be solved by transforming to magnetic coordinates. ("Magnetic coordinates" are flux coordinates with straight field lines: $\mathbf{B} \cdot \nabla \psi = 0$;

$\mathbf{B} \cdot \nabla \theta / \mathbf{B} \cdot \nabla \phi$ constant on the flux surface $= \iota(\psi)$.) Let $\mu \equiv j_{\parallel} / B$. In magnetic coordinates Eq. (2) can be rewritten

$$\frac{\partial \mu}{\partial \phi} + \iota \frac{\partial \mu}{\partial \theta} = -\frac{\nabla \cdot \mathbf{j}_{\perp}}{B^{\phi}}, \; B^{\phi} \equiv \mathbf{B} \cdot \nabla \phi. \tag{4}$$

Fourier transforming in θ and ϕ gives

$$(nN - \iota m)\mu_{nm} = -(\frac{\nabla \cdot \mathbf{j}_{\perp}}{B^{\phi}})_{nm}, \tag{5}$$

where n is the toroidal mode number per period, N is the number of periods, and m is the poloidal mode number. The $m = 0$, $n = 0$ Fourier coefficient, μ_{00}, is the constant of integration for Eq. (4), and it is determined by the profile of the net current.

In a stochastic magnetic field, Eq. (4) picks up an additional term:

$$\frac{\partial \mu}{\partial \phi} + \iota(\psi)\frac{\partial \mu}{\partial \theta} + \frac{\delta B^{\psi}}{B^{\phi}}\frac{\partial \mu}{\partial \psi} = -\frac{\nabla \cdot \mathbf{j}_{\perp}}{B^{\phi}}. \tag{6}$$

The corresponding homogeneous equation is mathematically equivalent to that for the collisionless Vlasov equation in the presence of electrostatic turbulence,

$$\frac{\partial f}{\partial t} + \mathrm{v}\frac{\partial f}{\partial x} + \frac{q}{m}\delta E\frac{\partial f}{\partial \mathrm{v}} = 0. \tag{7}$$

To go from Eq. (6) to Eq. (7), we assume that ι is monotonic in the region of interest so that we can adopt it as our radial variable, and we identify $\mu \to f,\; \phi \to t,\; \iota \to \mathrm{v},\; \theta \to \mathrm{x}$.

The relationship between Eqs. (6) and (7) allows us to apply the results of resonance-broadening theory.[7] We conclude that the perturbation to the magnetic field has only a small effect on the nonresonant Fourier terms in Eq. (5), but that the near-resonant Fourier components see a resonance broadening effect that causes the magnitude of μ_{nm} to remain bounded near resonances. This is what we would expect, because the nonresonant Fourier components have relatively short wavelengths along the magnetic field, so they see relatively little effect from the slow radial diffusion of the magnetic field lines, whereas the near-resonant Fourier components have long wavelengths along the field lines, and they see a phase-mixing effect due to the radial diffusion.

The relationship between Eqs. (6) and (7), and its corollaries for equilibria in stochastic magnetic fields, are discussed in more detail in reference [8]. We will have more to say about the solution of Eq. (6) for the cases at hand in the next section.

5. Equilibrium Solutions and Chaotic Field Line Trajectories

Figure 2 shows Poincare plots for the PIES equilibrium solutions with $I_{cc} = -2.5\mathrm{kA}$ and $I_{cc} = 0$. Although the value of $\langle \beta \rangle$ is substantially higher in the $I_{cc} = -2.5\mathrm{kA}$ shot ($\langle \beta \rangle \approx 2.7\%$ vs. $\langle \beta \rangle \approx 1.8\%$), the stochastic region is actually somewhat broader in the $I_{cc} = 0$ case. The last nested flux surface is at $r/a \approx 0.65$ in Fig. 1, and at $r/a \approx 0.59$ in Fig. 2, where r/a is measured along the outer midplane at $\phi = 0$. In a previous study of these two configurations where zero net current was assumed, two sequences of equilibria were calculated with varying β, fixed pressure profile and coil currents.[2] It was found that the widths of the edge stochastic regions decrease with decreasing β, going to zero below a β threshold. The calculations found that the width of the stochastic region is smaller for the
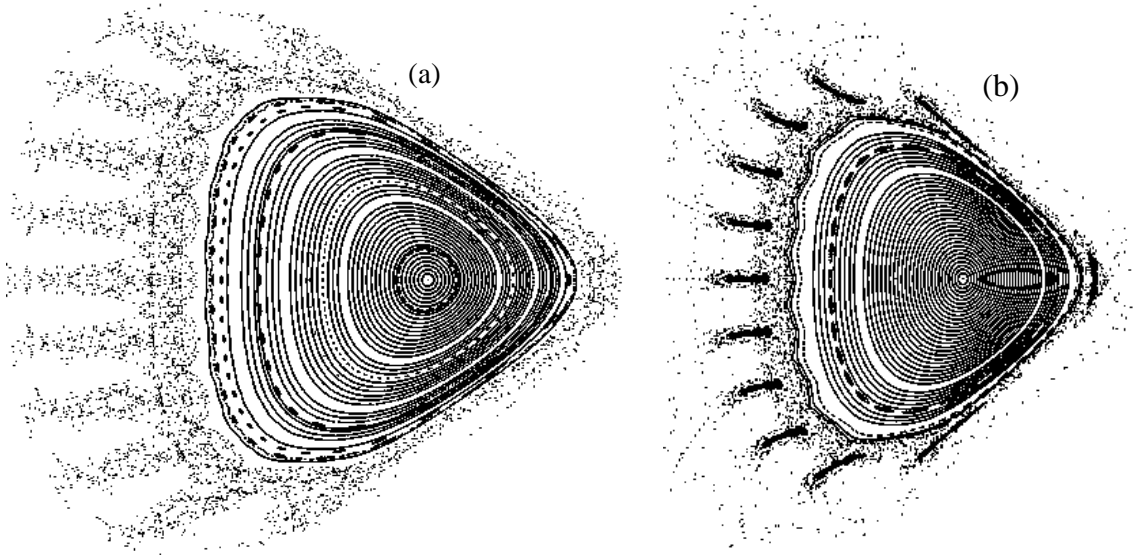
FIG 2.Poincare plots for equilibrium solutions with (a) I_{cc} = -2.5kA, $\langle\beta\rangle \approx 2.7\%$, (b)$I_{cc}$ = 0, $\langle\beta\rangle \approx 1.8\%$.

I_{cc} = -2.5kA configuration for each value of β, and that the threshold at which the width of the stochastic region goes to zero is also larger for that case.

To examine the chaotic field line trajectories, we plot polar coordinates ρ and θ as a function of ϕ along the field lines. The (ρ, θ) coordinate system used for this purpose has been defined in terms of the equilibrium solution obtained by the VMEC code, which uses a representation for the magnetic field that assumes nested flux surfaces. The radial coordinate ρ is taken to be constant on VMEC flux surfaces, and to measure the distance of the VMEC flux surface from the magnetic axis along the θ =0 ϕ=0 line. The angular coordinate θ is identical to the VMEC angular coordinate, with θ=0 on the inner midplane.

Figure 3 shows plots of ρ and θ vs.ϕ for the I_{cc} = -2.5kA, $\langle\beta\rangle \approx 2.7\%$ configuration. Figure 3a shows a relatively smooth curve punctuated by rapid, erratic radial excursions. The field line

FIG. 3. (a) ρ vs.ϕ, and (b) θ vs.ϕ along a chaotic field line trajectory.
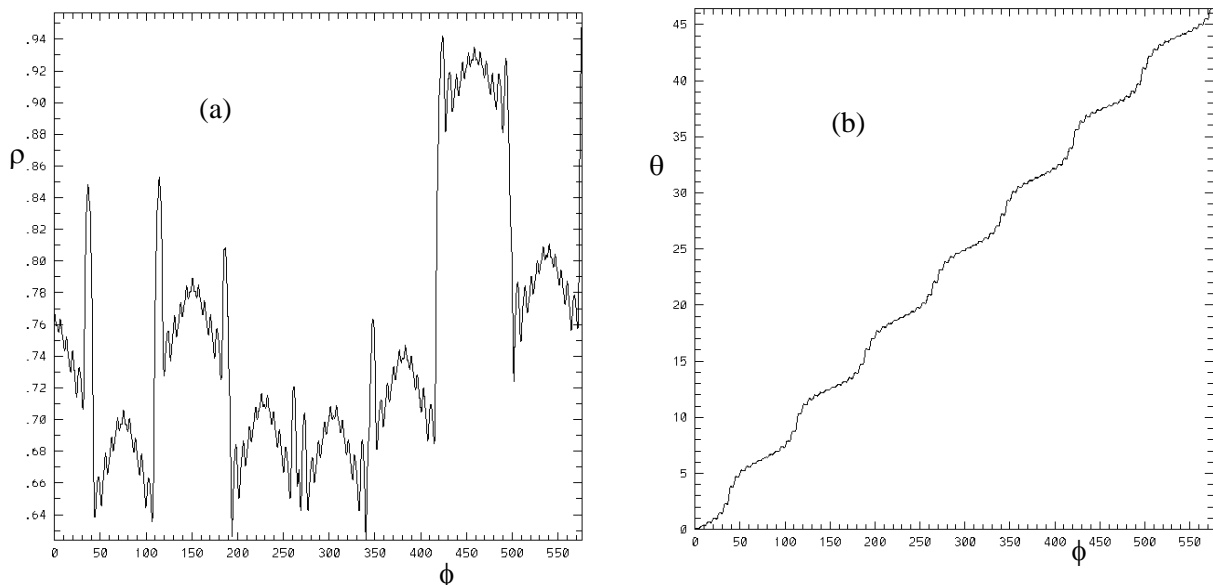
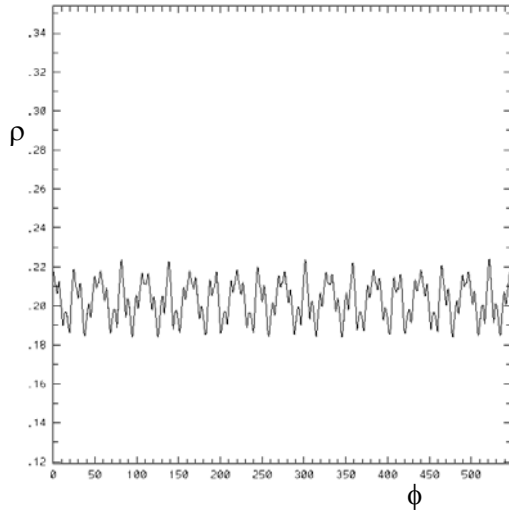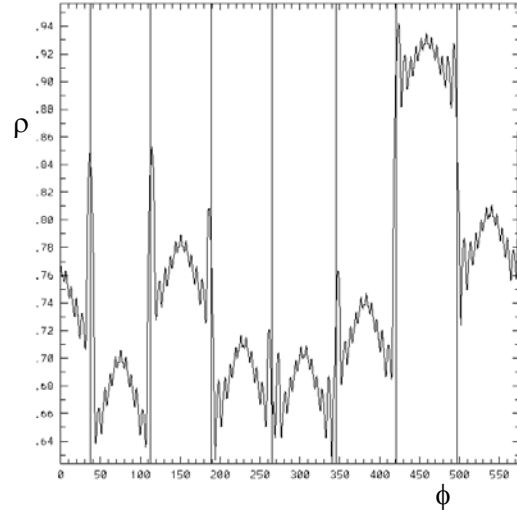FIG. 4. ρ vs. ϕ for a field line on a flux surface.

FIG. 5. Plot of fig. 3a, with vertical lines added at crossings of outer midplane.

following was terminated for this case when one of the large radial excursions caused the field line to exit the plasma. Figure 4 shows ρ vs. ϕ for a field line lying on a flux surface. The plot does not exhibit such radial jumps, and the radial excursion of the trajectory remains bounded.

The abrupt radial excursions in Fig.3a occur when the field line crosses the outboard midplane, $\theta = \pi$. To demonstrate this, Fig. 5 shows the same ρ vs. ϕ plot as Fig. 3a, with additional vertical lines placed at the crossings of the outer midplane. It can be seen that the radial jumps occur only near the outer midplane, and that, furthermore, erratic behavior occurs each time the trajectory crosses the outer midplane. The value of ρ on each smooth segment of the curve between the radial jumps returns to approximately its initial value as the field line returns to the $\theta = \pi$ region. The behavior of the field line shown in Figs. 3 and 5 is typical of the field lines in the stochastic region. The field lines behave as if, in effect, the flux surfaces in the stochastic region have been punctured near the outer midplane but remain intact elsewhere. This differs from the conventional picture of field lines in a stochastic region, where the field lines are everywhere diffusing radially. (See, e.g., [5].)

With this additional information about the chaotic field line trajectories, we revisit the calculation of Pfirsch-Schlüter currents discussed in the previous section. The field lines approximately follow the unperturbed surfaces, except near the outer midplane. The wavelength of a mode having mode numbers (n,m) is $nN-\iota m$. The connection length between encounters with the outer midplane is $2\pi/(\iota R)$. For Fourier modes having wavelength short compared to the conection length, it is reasonable to do a local analysis, Eq. (5). For modes having wavelength long compared to the connection length, phase mixing gives the corresponding solutions of Eq. (6) a small amplitude. Thus we recover the resonance-broadening effect discussed earlier.

6. Diffusion Coefficients

Heat is carried along the field lines primarily by the electrons. (Particle transport is more complicated because of the development of radial electric fields.) We evaluate first the magnetic field line diffusion, and then the heat transport.
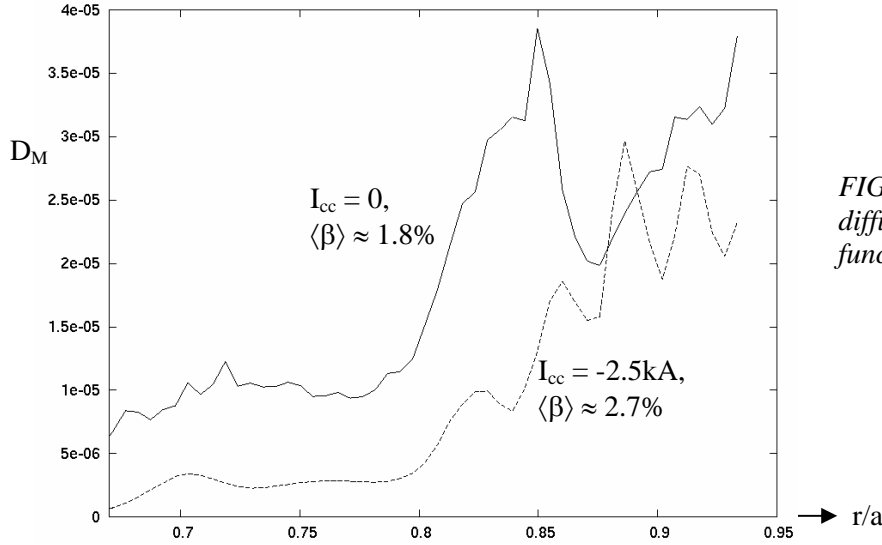
FIG. 6. Calculated magnetic diffusion coefficient as a function of r/a.

The magnetic diffusion coefficient measures the mean square radial displacement of a magnetic field line as a function of the distance along the field line. Given the characterization of the chaotic field line trajectories developed in the previous section, we can estimate the magnetic diffusion coefficient as $D_M \approx \left\langle \left(\Delta r\right)^2 \right\rangle / L_c$, where L_c is the distance between encounters with the outer midplane, and $\left\langle \left(\Delta r\right)^2 \right\rangle$ is the mean square radial jump experienced by a field line as it crosses the outer midplane. We evaluated this quantity by following 100 field lines launched at different values of ϕ once around the torus in the poloidal direction, and measuring the radial jump relative to the underlying unperturbed flux surfaces. (We have verified that increasing the number of field lines followed by a factor of 10 does not have an appreciable effect on the calculated diffusion coefficient.) Fig 6 is a plot of the calculated magnetic diffusion coefficient for the two shots we are studying. The diffusion coefficient is substantially larger for the shot with $I_{CC} = 0$ than for that with $I_{CC} \approx -2.5$ kA. This is consistent with the observation that the latter shot achieves a higher value of $\langle \beta \rangle$ than the former for the same injected neutral beam power.

Figure 7 shows the reconstructed pressure profiles for the shots with $I_{CC} \approx -2.5$ kA and $I_{CC} = 0$. The latter displays a decreased pressure gradient in the outer region, again consistent with the picture that the relatively larger magnetic diffusion coefficient in this shot is having a deleterious effect on confinement.

To estimate the contribution of the field line stochasticity to the energy transport, we must estimate the energy carried along the stochastic field lines by the electrons. As it follows a field line, each electron experiences a radial jump when the field line crosses the outer midplane. The radial diffusion coefficient of the electrons is $\chi_{stoch} \approx \left\langle \left(\Delta r\right)^2 \right\rangle / \tau_c$, where τ_c is the time it takes for an electron to follow one traversal of a field line in the poloidal direction. The electron mean free path is small compared to L_c, so $\tau_c = L_c^2 / \chi_e$, where χ_e is the diffusion coefficient for the electrons along the field lines, $\chi_e \approx (v_{te}/\nu_{ei})^2 \nu_{ei} \approx v_{te}^2 / \nu_{ei} \propto T_e^{5/2} / n_e$. The calculated thermal transport is very sensitive to the electron temperature. Within the uncertainties in the electron temperature, χ_{stoch} is estimated to be of order 1 m^2/sec, which is consistent with the observations.
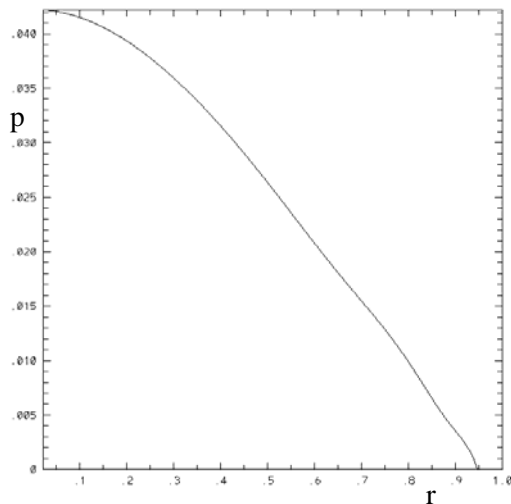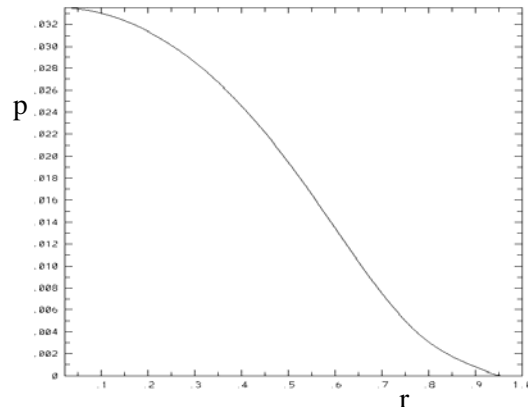
FIG. 7. Reconstructed pressure profiles for (a) I_{cc} = -2.5kA, $\langle\beta\rangle \approx 2.7\%$, (b)$I_{cc}$ = 0. $\langle\beta\rangle \approx 1.8\%$.. (a = .95)

7. Discussion

W7AS experiments have found that the magnitude of the divertor control coil current has a strong effect on the achievable β. There is no evidence that instabilities are playing a role in degrading the plasma confinement in these experiments. The divertor control coil has been designed to provide control over the resonant magnetic field near the plasma edge, and it is calculated to have little effect on ι, on neoclassical ripple transport, or on magnetic axis shift.

Three-dimensional equilibrium calculations for W7AS find that a region of chaotic field line trajectories emerges at the plasma edge when β exceeds a threshold, and that the stochastic region increases in width as β is increased. The field lines in the stochastic region behave as if the flux surfaces are broken only locally near the outer midplane and are preserved elsewhere. The emergence of the stochastic region is consistent with the conventional wisdom that the strong compression and distortion of the 3D flux surfaces due to the Shafranov shift can break the flux surfaces as beta is increased. A simplified, analytically tractable model of this effect finds that the increase in beta leads to an increasingly strong coupling between resonant Fourier components and low order nonresonant Fourier components of the magnetic field.[9]

Equilibrium reconstruction indicates the presence of a substantial pressure gradient in the stochastic region. To solve for the Pfirsch-Schlüter currents in this region, we use techniques developed for the resonance broadening theory of electrostatic turbulence. Equilibrium calculations which differ in the magnitude of the control coil current find contributions of the field line stochasticity to the diffusion coefficients which are consistent with the observed differences in the achievable β and the reconstructed pressure profiles.

[1] L. Spitzer, Phys. Fluids **1**, 253 (1958).
[2] M.C. Zarnstorff *et al*, 21st IAEA Fusion Energy Conference, Vilamoura, 2004. EX/3-4.
[3] A. Weller *et al*, 15th International Stellarator Workshop, Madrid, 2005.
[4] A. Reiman and H. Greenside, Compt. Phys. Commun. **43**, 157 (1986).
[5] See e.g. A. Rechester and M. Rosenbluth, Phys. Rev. Lett. **40**, 38 (1978).
[6] S.P. Hirshman et al., Comput. Phys. Commun. **43** (1986) 143.
[7] See e.g. J. Krommes, Phys. Reports **360**, 1 (2002), and references therein.
[8] A. Reiman and J. Krommes, to be published.
[9] A. Reiman and A. Boozer, Phys. Fluids **27**, 2446 (1984).